J = 4.7 Hz), 8.68 (4H, d, J = 8.0 Hz), 8.00 (4H, d, J = 8.6 Hz), 7.88 (4H, dt, J = 7.6 Hz, J = 1.7 Hz), 7.62 (2H, s), 7.41–7.36 (8H, m), 1.53–1.46 (14H, m), 1.33–1.23 (24H, m). ^{13}C NMR (300 MHz, $CDCl_3$): δ [ppm] = 156.1, 152.4, 149.2, 136.9, 128.5, 123.8, 122.2, 121.4, 118.8, 70.1, 31.9, 29.6, 29.3, 26.0.

1f: Yield: 80 %. FABMS: *m/e* 1062; $C_{72}H_{80}N_6O_2$ requires *m/e* 1061.4. m.p.: 192 °C. ^{1}H NMR (300 MHz, $CDCl_3$): δ [ppm] = 8.83 (4H, s), 8.76–8.71 (4H, m), 8.69 (4H, d, J = 8.0 Hz), 8.01 (4H, d, J = 8.3 Hz), 7.90 (4H, dt, J = 7.7 Hz, J = 1.1 Hz), 7.79 (4H, d, J = 8.6 Hz), 7.36 (4H, m), 7.09 (2H, s), 1.75–1.70 (4H, m), 1.53–1.19 (40H, m), 0.84–0.81 (6H, m). ^{13}C NMR (300 MHz, $CDCl_3$): δ [ppm] = 156.4, 156.0, 150.5, 150.0, 149.2, 139.3, 136.8, 130.1, 116.9, 123.8, 121.4, 118.8, 116.3, 69.9, 31.9, 29.7, 29.6, 29.4, 29.3, 26.1, 22.7, 14.1.

1g: Yield: 70 %. FABMS: *m/e* 954; $C_{66}H_{44}N_6O_2$ requires *m/e* 953.1. m.p.: 137 °C. ^{1}H NMR (300 MHz, $CDCl_3$): δ [ppm] = 8.83 (4H, s), 8.77 (4H, dd, J = 1.7 Hz, J = 0.9 Hz), 8.69 (4H, d, J = 8.0 Hz), 8.00 (4H, d, J = 8.4 Hz), 7.90 (4H, dt, J = 7.7 Hz, J = 1.8 Hz), 7.77 (4H, d, J = 8.4 Hz), 7.39–7.32 (14H, m), 7.17 (2H, s), 5.10 (4H, s). ^{13}C NMR (300 MHz, $CDCl_3$): δ [ppm] = 156.4, 156.0, 150.3, 149.2, 136.8, 130.1, 128.5, 127.8, 127.2, 127.0, 123.8, 121.4, 118.8, 117.3, 71.8.

1h: Yield: 73 %. FABMS: *m/e* 1006; $C_{71}H_{68}N_6$ requires *m/e* 1005.4. ^{1}H NMR (300 MHz, $CDCl_3$): δ [ppm] = 8.83 (4H, s), 8.77–8.74 (4H, m), 8.68 (4H, d, J = 6.0 Hz), 8.05 (4H, d, J = 6.3 Hz), 7.90 (4H, dt, J = 7.8 Hz, J = 1.8 Hz), 7.83 (6H, d, J = 6.3 Hz), 7.70–7.67 (4H, m), 7.38 (4H, ddd, J = 2.7 Hz, J = 1.2 Hz, J = 0.8 Hz,), 2.14–2.09 (4H, m), 1.23–1.11 (18H, m), 0.80 (8H, m). ^{13}C NMR (300 MHz, $CDCl_3$): δ [ppm] = 156.4, 156.1, 151.9, 149.8, 149.2, 142.4, 140.4, 139.4, 137.2, 136.9, 127.7, 127.7, 126.1, 123.8, 121.5, 121.4, 120.2, 118.7, 55.4, 40.4, 31.8, 30.0, 29.2, 23.9, 22.6, 14.0.

Received: February 17, 2003
Final version: July 2, 2003

[1] a) J. H. Burroughes, D. D. C. Bradley, A. R. Brown, R. N. Marks, K. Mackay, R. H. Friend, P. L. Burn, A. B. Holmes, *Nature* **1990**, *347*, 539. b) D. Braun, A. J. Heeger, *Appl. Phys. Lett*. **1991**, *58*, 1982. c) C. T. Wong, W. K. Chan, *Adv. Mater.* **1999**, *11*, 455. d) W. Y. Ng, W. K. Chan, *Adv. Mater.* **1997**, *9*, 716. e) A. Kraft, A. C. Grimsdale, A. B. Holmes, *Angew. Chem. Int. Ed*. **1998**, *37*, 402.

[2] S.-C. Chang, J. Bharathan, Y. Yang, R. Helgeson, F. Wudl, M. B. Ramey, J. R. Reynolds, *Appl. Phys. Lett.* **1998**, *72*, 2561.

[3] J. C. Scott, J. H. Kaufman, P. J. Brock, R. DiPietro, J. Salem, J. A. Goitia, *J. Appl. Phys.* **1996**, *79*, 2745.

[4] U. Scherf, E. J. W. List, *Adv. Mater*. **2002**, *14*, 477.

[5] a) C. Xia, R. C. Advincula, *Marcomolecules* **2001**, *34*, 5854. b) V. N. Bliznyyuk, S. A. Carter, J. C. Scott, G. Klarner, R. D. Miller, D. C. Miller, *Marcomolecules* **1999**, *32*, 361. c) G. Klarner, J. I. Lee, V. Y. Lee, E. Chan, J. P. Chen, A. Nelson, D. Markiewicz, R. Siemens, J. C. Scott, R. D. Miller, *Chem. Mater*. **1999**, *11*, 1800.

[6] a) M. A. Baldo, D. F. O'Brien, M. E. Thompson, S. R. Forrest, *Phys. Rev. B* **1999**, *60*, 14 422. b) S. Lamansky, P. Djurovich, D. Murphy, F. Abdel-Razzaq, H. E. Lee, C. Adachi, P. E. Burrows, S. R. Forrest, M. E. Thompson, *J. Am. Chem. Soc.* **2001**, *123*, 4304. c) Y. Y. Lin, S. C. Chan, M. C. W. Chan, Y. J. Hou, N. Y. Zhu, C. M. Che, Y. Liu, Y. Wang, *Chem. Eur. J.* **2003**, *9*, 1263. d) W. Lu, B. X. Mi, M. C. W. Chan, Z. Hui, N. Y. Zhu, S. T. Lee, C. M. Che, *Chem. Commun.* **2002**, 206. e) S. C. Chan, M. C. W. Chan, C. M. Che, Y. Wang, K. K. Cheung, N. Y. Zhu, *Chem. Eur. J.* **2001**, *7*, 4180.

[7] a) S. C. Yu, X. Gong, W. K. Chan, *Macromolecules* **1998**, *31*, 5639. b) S. C. Yu, S. Hou, W. K. Chan, *Macromolecules* **1999**, *32*, 5251. c) S. C. Yu, S. Hou, W. K. Chan, *Macromolecules* **2000**, *33*, 3259. d) W. K. Chan, X. Gong, W. Y. Ng, *Appl. Phys. Lett.* **1997**, *71*, 2919.

[8] a) W. Y. Ng, X. Gong, W. K. Chan, *Chem. Mater*. **1999**, *11*, 1165. b) K. D. Ley, C. E. Whittle, M. D. Bartberger, K. S. Schanze, *J. Am. Chem. Soc.* **1997**, *119*, 3423. c) A. A. Farah, W. J. Pietro, *Polym. Bull*. **1999**, *43*, 135. d) J. S. Wilson, A. S. Dhoot, A. J. A. B. Seeley, M. S. Khan, A. Köhler, R. H. Friend, *Nature* **2001**, *413*, 828.

[9] a) U. S. Schubert, C. Eschbaumer, *Angew. Chem. Int. Ed.* **2002**, *41*, 2892. b) U. S. Schubert, M. Heller, *Chem. Eur. J.* **2001**, *7*, 5253. c) W. Goodall, J. A. Gareth, *Chem. Commun*. **2001**, 2514. d) S. Kelch, M. Rehahn, *Chem. Commun*. **1999**, 1123.

[10] R. Dobrawa, F. Würthner, *Chem. Commun*. **2002**, 1878.

[11] M. Kimura, T. Horai, K. Hanabusa, H. Shirai, *Adv. Mater*. **1998**, *10*, 459.

[12] R. F. Heck, *Org. React*. **1982**, *27*, 345.

[13] N. W. Alcock, P. R. Barker, J. M. Haider, M. J. Hannon, C. L. Painting, Z. Pikramenou, E. A. Plummer, K. Rissanen, P. Saarenketo, *J. Chem. Soc., Dalton Trans.* **2000**, 1447.

[14] F. Loiseau, C. D. Pietro, S. Serroni, S. Campagna, A. Licciardello, A. Manfredi, G. Pozzi, S. Quici, *Inorg. Chem*. **2001**, *40*, 4901.

[15] J. C. de Mello, H. F. Wittmann, R. H. Friend, *Adv. Mater*. **1997**, *9*, 230.

[16] a) U. S. Schubert, O. Hien, C. Eschbaumer, *Macromol. Rapid Commun*. **2000**, *21*, 1156. b) B. Liu, W. L. Yu, Y. H. Lai, W. Huang, *Macromolecules* **2002**, *35*, 4975.

Synthesis of Hierarchical Superstructures Consisting of $BaCrO_4$ Nanobelts in Catanionic Reverse Micelles**

By *Hongtao Shi*, *Limin Qi*,* *Jiming Ma*, *Humin Cheng*, and *Buyao Zhu*

One-dimensional (1D) nanostructures, such as nanotubes, nanowires, nanorods, and nanobelts, have stimulated intensive interest owing to their unique applications in mesoscopic physics and the fabrication of nanoscale devices.[1–3] Many recent efforts have focused on the integration of 1D nanoscale building blocks into two- and three-dimensional (2D/3D) ordered superstructures or complex functional architectures, which is a crucial step toward realization of functional nanosystems.[4–7] For example, ordered nanorod arrays were obtained by the self-assembly of preformed uniform nanorods through hydrophobic interaction,[4] DNA hybridization,[8] and a Langmuir–Blodgett technique,[9] whereas multi-armed[5] and radially aligned[10] semiconductor nanorods were fabricated by solution-growth methods. Notably, the self-organized crystal growth of a variety of novel hierarchical nanostructures made of nanowires has been achieved recently; examples include the growth of ZnO nanobridges, nanosnails, and nanocombs by a vapor-transport and condensation technique,[11] and the polymer-directed synthesis of penniform $BaWO_4$ nanostructures in reverse micelles.[12] As a new family of 1D nanostructures, nanobelts have received much attention because of their unique properties and potential applications in building functional nanodevices;[13,14] however, there are few reports concerning the assembly of nanobelts into hierarchical nanostructures.[15] It remains a significant challenge to develop facile, mild, and effective methods for creating hierarchical architectures assembled from inorganic nanobelts.

Reverse micelles and microemulsions have been widely used as soft colloidal templates for controlling the size and shape of inorganic nanocrystals.[16] Recently, reverse micelles formed by mixed surfactants have turned out to be promising nanostructured media for the controlled synthesis of 1D nanostructures.[17,18] Specifically, high-aspect-ratio, ultrathin $BaWO_4$ nanowires were produced using the so-called catanionic re-

[*] Prof. L. Qi, H. Shi, Prof. J. Ma, Prof. H. Cheng, Prof. B. Zhu
State Key Laboratory for Structural Chemistry
of Stable and Unstable Species
College of Chemistry, Peking University
Beijing 100871 (China)
E-mail: liminqi@chem.pku.edu.cn

[**] This work was supported by the NSFC (20003001, 20233010), the Special Fund of MOE, China (200020), and the Doctoral Program Foundation of MOE, China.

 DOI: 10.1002/adma.200305625

ADVANCED MATERIALS

verse micelles that were formed by mixed cationic–anionic surfactants.[18] It is known that the composition conditions of reverse micelles largely influence the structures of the surfactant aggregates as well as the size and shape of the final nanocrystals. For the unique catanionic reverse micelle system, the molar ratio (r) between the mixed anionic and cationic surfactants is expected to play a key role in the synthesis of 1D nanostructures. Currently, $BaCrO_4$ has been widely used as a model system for the synthesis and self-assembly of 1D nanoscale building blocks. For instance, $BaCrO_4$ nanorods obtained in anionic reverse micelles were assembled into ordered nanorod arrays,[4,9] whereas $BaCrO_4$ nanofibers were synthesized and self-assembled into hierarchical superstructures by polymer controlled crystallization.[19] Herein, we report the synthesis of a variety of novel $BaCrO_4$ nanostructures, such as nanowires, nanobelts, and tree-like superstructures consisting of nanobelts, in catanionic reverse micelles by simply changing the mixing ratio r. To the best of our knowledge, this is the first report on the synthesis of hierarchical, tree-like superstructures consisting of inorganic nanobelts.

The synthesis of $BaCrO_4$ nanostructures was simply achieved by the reaction of barium and chromate ions solubilized in the catanionic micelles consisting of water, decane, undecylic acid, and decyl amine, where the cationic surfactant was produced by the protonation of the amine by undecylic acid.[18] X-ray diffraction (XRD) studies indicated that all the products were crystalline $BaCrO_4$ with an orthorhombic unit cell (Joint Committee on Powder Diffraction Standards, JCPDS, card: 15-376, $a = 0.9105$ nm, $b = 0.5541$ nm, $c = 0.7343$ nm). Figures 1a,b present typical transmission electron microscopy (TEM) images of the product obtained at 30 °C and at a mixing ratio $r = 1$, i.e., in the presence of equimolar undecylic acid and decyl amine, which shows the formation of bundles of $BaCrO_4$ nanowires with lengths 1.2–1.5 μm and a diameter of about 6 nm. The related electron diffraction (ED) pattern shows fairly broad rings, corresponding to the orthorhombic $BaCrO_4$ structure, indicating that the $BaCrO_4$ nanowires were not well-crystallized under this condition. When r was decreased to 0.4, i.e., in the presence of excess decyl amine, $BaCrO_4$ nanowire arrays resembling crossed haystacks were obtained (Fig. 1c,d). The nanowires, which were 1.5–2.0 μm in length and 10–15 nm in diameter, were well-crystallized orthorhombic $BaCrO_4$ according to the sharp rings in the related ED pattern (inset of Fig. 1c). The ED pattern of nearly parallel nanowires (inset of Fig. 1d) exhibits diffraction spots rather than rings and only (00l) spots can be observed along the wire length axis, indicating that each nanowire is a single crystal with the c axis along the length axis.

If the undecylic acid/decyl amine molar ratio r was increased to larger than 1, i.e., in the presence of excess undecylic acid, $BaCrO_4$ nanobelts as well as their unique assemblies showing tree-like superstructures can be obtained. At $r = 1.4$, the obtained product was bundles of $BaCrO_4$ nanobelts with a length about 1.6 μm (Fig. 2a). Enlarged images showing twisted and straight nanobelts (Figs. 2b,c) suggested that the nanobelts were about 65 nm in width and about 6 nm in thickness. The ED pattern related with nearly parallel, straight nanobelts exhibited diffraction spots predominantly corresponding to the [010] zone of the orthorhombic $BaCrO_4$ structure with (00l) spots along the length direction, indicating

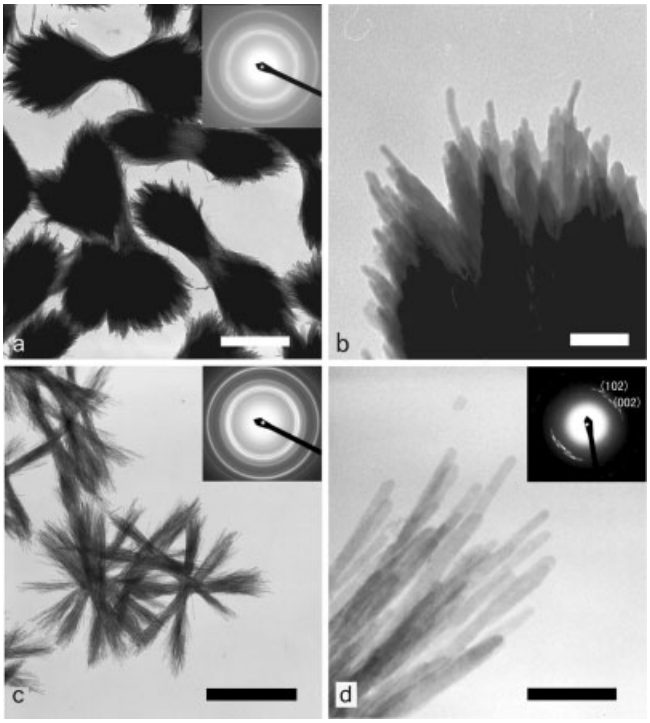

Fig. 1. TEM images of $BaCrO_4$ nanowires formed at 30 °C and $r = 1$ (a,b) and $r = 0.4$ (c,d). Insets show the corresponding ED patterns. Scale bars: a) 500 nm, b) 50 nm, c) 1 μm, d) 100 nm.

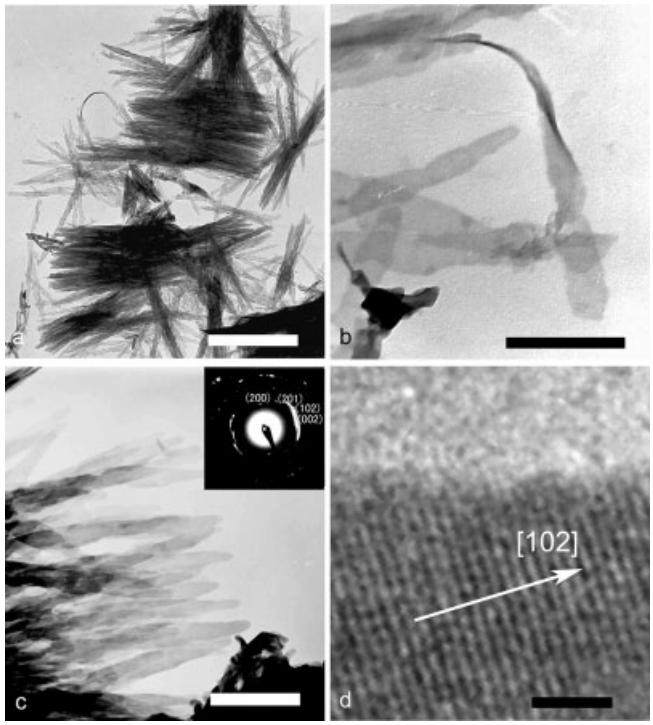

Fig. 2. TEM images of $BaCrO_4$ nanobelts formed at 30 °C and $r = 1.4$. Inset shows the corresponding ED pattern. Scale bars: a) 1 μm, b,c) 200 nm, d) 2 nm.

that each nanobelt was a single crystal with the *c* axis along the length direction and the *a* axis along the width direction. The high resolution TEM (HRTEM) image shown in Figure 2d confirmed the single-crystalline nature of the $BaCrO_4$ nanobelts.

When *r* was increased to 1.7:1, hierarchical, tree-like $BaCrO_4$ superstructures (~10 μm in length), which consisted of branches with numerous, nearly parallel nanoleaflets grown on two opposite sides, were produced (Fig. 3a). The branches were about 40 nm in width and the nanoleaflets grown on the branches were about 100 nm in length, 20 nm in width

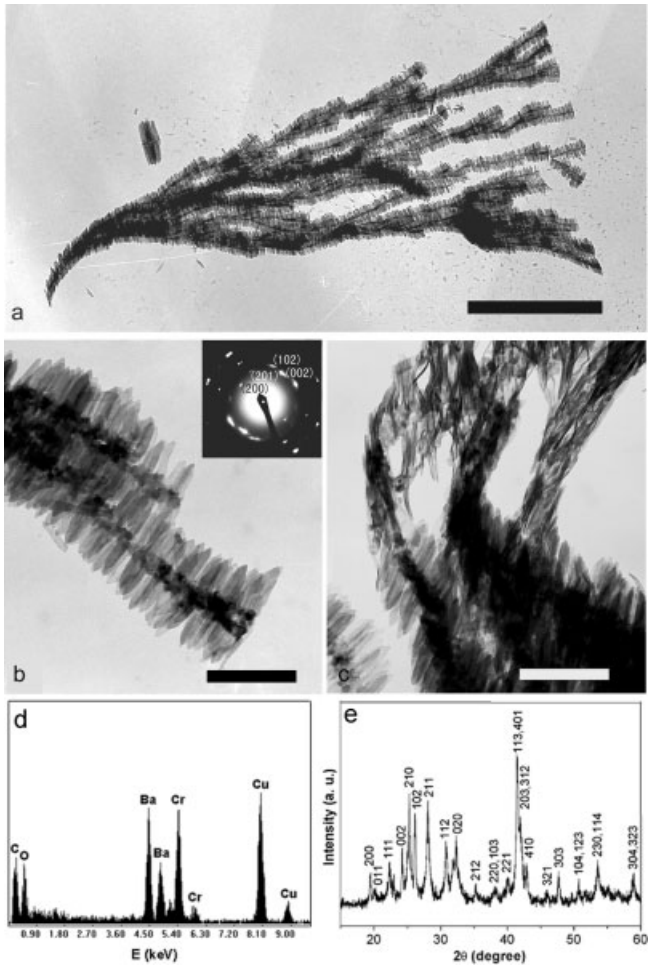

Fig. 3. TEM images (a–c), EDS spectrum (d), and XRD pattern (e) of tree-like $BaCrO_4$ superstructures formed at 30 °C and $r = 1.7$. Inset shows the corresponding ED pattern. Scale bars: a) 2 μm, b,c) 200 nm.

(Fig. 3b). The twisted branches shown in Figure 3c clearly revealed that the nanoleaflets were nanobelts with a thickness of about 4 nm. The ED pattern corresponding to a single branch containing leaflets indicated that the whole branch was orthorhombic $BaCrO_4$ crystals with the *a* axis along the length direction and the *c* axis along the width direction, which suggested that the nanoleaflets grew in length along the *c* axis and width along the *a* axis, consistent with the growth direction of the $BaCrO_4$ nanobelts obtained at $r = 1.4$. The related energy-dispersive X-ray spectroscopy (EDS) spectrum (Fig. 3d) and the XRD spectrum (Fig. 3e) confirmed that the tree-like product was pure $BaCrO_4$ of the orthorhombic structure. It is noted that $BaCrO_4$ nanofilament bundles and nanorod arrays have been produced in $Ba(AOT)_2$ reverse micelles;[4] however, $BaCrO_4$ nanobelts, as well as their superstructures, have not been obtained so far.

If *r* was further increased to 2, bare-tree-like $BaCrO_4$ superstructures showing self-similarity were obtained (Fig. 4a). An enlarged image (Fig. 4b) revealed that there were no nanoleaflets grown on the branches but there were secondary trees grown on the sharp growth front of the primary tree, which is

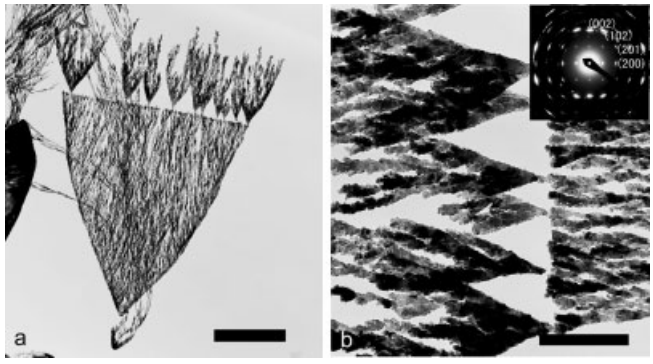

Fig. 4. TEM images of bare-tree-like $BaCrO_4$ superstructures formed at $r = 2$. Inset shows the corresponding ED pattern. Scale bars: a) 2 μm, b) 500 nm.

reminiscent of the bundles of $BaCrO_4$ nanofibers crystallized in aqueous solutions of polymers.[19a] The related ED pattern indicated that the bare branches were $BaCrO_4$ crystals grown along the [100] direction, similar to the growth direction of the branches containing nanoleaflets shown in Figure 3.

The growth process of the tree-like $BaCrO_4$ superstructures containing nanoleaflets, which were obtained at $r = 1.7$ after 24 h of aging, were followed by examining the earlier stages of their formation. After 5 min of aging, tree-like superstructures with bare branches formed (Figs. 5a,b), which were $BaCrO_4$ crystals grown along the [100] direction, as revealed by the related ED pattern. At an aging time of 15 min, nanoleaflets about 20 nm in length grew perpendicularly on two opposite sides of each branch (Fig. 5c). After 8 h of aging, many nanoleaflets had grown up to about 100 nm in length but there were still some shorter, growing nanoleaflets (Fig. 5d). If the aging time was further increased to 24 h, almost all the nanoleaflets grew up to about 100 nm as shown in Figure 3, and then the leaflet length stayed essentially unchanged with time. The whole growth process was essentially similar to that of the penniform $BaWO_4$ nanostructures reported previously.[12]

It has been suggested that emergent nanostructures with complex form and hierarchy may result from mesoscale transformation of hybrid inorganic–organic building blocks formed through strong binding interactions between adsorbed organic molecules and the inorganic surface.[20] In the current situation, the formation of $BaCrO_4$ nanobelts as well as their superstructures might involve a continuous supply of hybrid nanoparticle precursors to the growth sites of crystals under

ADVANCED MATERIALS

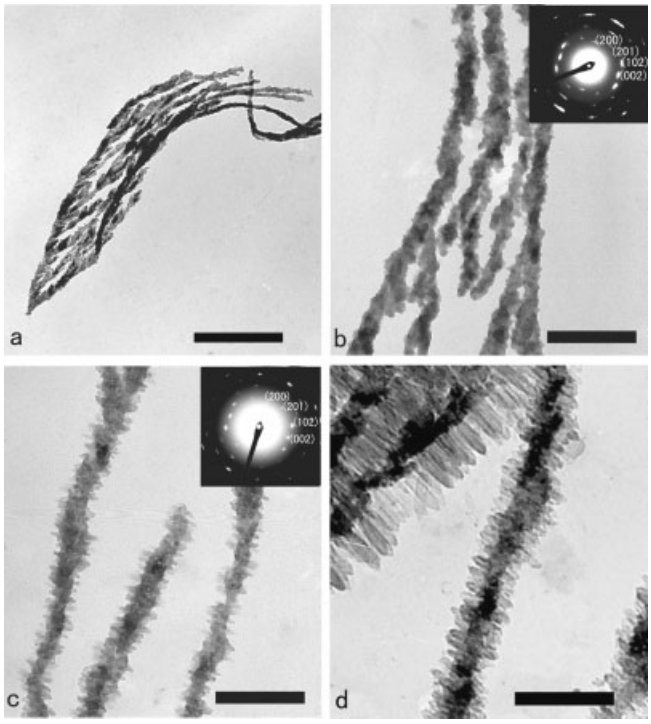

Fig. 5. TEM images of $BaCrO_4$ nanostructures obtained at earlier stages for the tree-like superstructures formed at 30 °C and $r = 1.7$. Aging time: a,b) 5 min, c) 15 min, d) 8 h. Insets show the corresponding ED patterns. Scale bars: a) 500 nm, b–d) 200 nm.

the direction of surfactant molecules. It has been documented that polycarboxylate can interact strongly with $BaCrO_4$ crystals due to the coordination interaction between carboxylate groups and the Ba^{2+} ions,[19] which indicates that $BaCrO_4$ could preferentially interact with or adsorb undecylic acid in the mixed catanionic surfactants. It is noted that the proportion of undecylic acid in the mixed surfactants film of the reverse micelles increases with increasing r, indicating that the distance between neighboring carboxylate groups in the interfacial film decreases with increasing r. It is reasonably assumed that the interfacial film with varied r values would preferentially adsorb on specific faces of the $BaCrO_4$ crystals due to interfacial molecular recognition and thus induce preferential crystal growth. For example, at $r = 1$ or $r < 1$, undecylic acid could preferentially adsorb on surfaces parallel to the c axis, resulting in the formation of $BaCrO_4$ nanowires along [001] direction. At $r = 1.4$, undecylic acid could preferentially adsorb on the (010) surface, resulting in the formation of $BaCrO_4$ nanobelts showing (010) top surface and grown along the [001] direction. When r was increased to 2, undecylic acid could preferentially adsorb on surfaces parallel to the a axis, resulting in the formation of tree-like $BaCrO_4$ superstructures with bare branches along the [100] direction. When r lies between 1.4 and 2, for instance, $r = 1.7$, undecylic acid could preferentially adsorb on surfaces parallel to the a axis at the beginning, resulting in the formation of bare branches. On crystal growing, the proportion of undecylic acid in the remaining mixed film could decrease due to preferential adsorption of undecylic acid on the crystals, leading to the growth of nanoleaflets showing (010) top surface as in the case of $r = 1.4$. However, the proposed mechanism is just a tentative explanation for the experimental results and remains to be demonstrated. It should be pointed out that some other factors should also be taken into account for a full understanding of the mechanism. For example, variation of r would considerably affect the micellar structures, such as the packing density of the interfacial film, which would affect the film elasticity and the area per molecule in the film that is closely related to the distance between neighboring carboxylate groups.

The reaction temperature has been found to play an important role in the morphological control of the $BaWO_4$ nanowires obtained in the catanionic reverse micelle system.[18] As expected, the temperature was also found to significantly influence the morphology of the obtained $BaCrO_4$ nanostructures. For example, when the reaction temperature was increased to 50 °C, only $BaCrO_4$ nanowires and their superstructures were obtained at all the studied mixing ratios. In particular, at $r = 1.7$, tree-like $BaCrO_4$ superstructures consisting of wire-like (rather than belt-like) nanoleaflets, which were elongated along the c axis and were about 200 nm in length and 6–8 nm in diameter, were obtained (Fig. 6). It is worth mentioning that hierarchical superstructures consisting

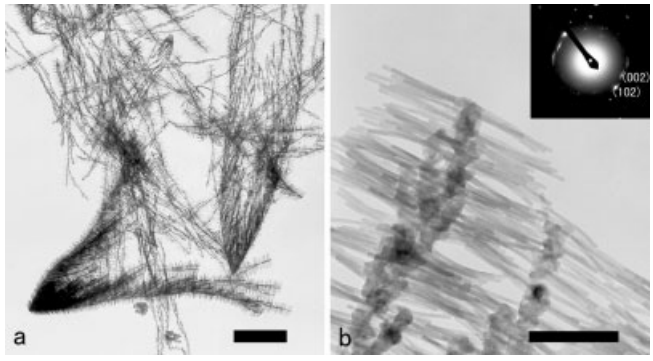

Fig. 6. TEM images of $BaCrO_4$ nanostructures formed at 50 °C and $r = 1.7$. Insets show the corresponding ED patterns. Scale bars: a) 2 μm, b) 200 nm.

of nanobelts of other barium salts including $BaMoO_4$ and $BaWO_4$ can also be obtained in this catanionic reverse micelle system under suitable conditions. Therefore, it is expected that such catanionic reverse micelle systems should be generally applicable for the synthesis of hierarchical superstructures consisting of inorganic nanobelts of many other materials systems.

In summary, a variety of novel $BaCrO_4$ nanostructures, such as nanowires, nanobelts, tree-like superstructures consisting of nanobelts, and bare-tree-like superstructures, have been synthesized in a unique catanionic reverse micelle system by simply changing the mixing ratio between the anionic and cationic surfactants. This synthetic method is very simple, mild, and controllable, and it provides a novel method for direct assembly of inorganic nanobelts into hierarchical superstructures.

Experimental

The selected catanionic reverse micelle system consists of water, decane, and a mixture of two surfactants: undecylic acid and decyl amine [18]. For the preparation of catanionic reverse micelles, undecylic acid and decyl amine were mixed with a certain molar ratio (r) in the liquid state under mild heating, leading to the formation of a catanionic surfactant mixture, which was present as a white solid at room temperature. The synthesis of $BaCrO_4$ nanostructures was simply achieved by the reaction of barium and chromate ions solubilized in the catanionic micelles. Typically, 0.782 g of the catanionic surfactant mixture was first dissolved in 2.5 mL of decane under mild heating. Then, 100 μL of 0.02 mol L^{-1} K_2CrO_4 solution was added with shaking, which was followed by the addition of 100 μL of 0.02 mol L^{-1} $BaCl_2$ and vigorous shaking. Finally, the resultant mixture was incubated for 24 h (unless otherwise stated) at 30 °C or 50 °C, resulting in the formation of yellow precipitates. The products were collected, washed with ethanol, and characterized by TEM (JEOL JEM-200CX apparatus), HRTEM (Hitachi H-9000HAR apparatus), and XRD (Rigaku Dmax-2000 apparatus with Cu Kα radiation).

Received: July 1, 2003

[1] J. Hu, T. W. Odom, C. M. Lieber, *Acc. Chem. Res.* **1999**, *32*, 435.
[2] G. R. Patzke, F. K. Krumeich, R. Nesper, *Angew. Chem. Int. Ed.* **2002**, *41*, 2446.
[3] Y. Xia, P. Yang, Y. Sun, Y. Wu, B. Mayers, B. Gates, Y. Yin, F. Kim, H. Yan, *Adv. Mater.* **2003**, *15*, 353.
[4] a) M. Li, H. Schnablegger, S. Mann, *Nature* **1999**, *402*, 393. b) M. Li, S. Mann, *Langmuir* **2000**, *16*, 7088.
[5] a) L. Manna, E. C. Scher, A. P. Alivisatos, *J. Am. Chem. Soc.* **2000**, *122*, 12700. b) S.-M. Lee, Y. Jun, S.-N. Cho, J. Cheon, *J. Am. Chem. Soc.* **2002**, *124*, 11244.
[6] N. I. Kovtyukhova, T. E. Mallouk, *Chem. Eur. J.* **2002**, *8*, 4354.
[7] Y. Wu, H. Yan, M. Huang, B. Messer, J. H. Song, P. D. Yang, *Chem. Eur. J.* **2002**, *8*, 1260.
[8] E. Dujardin, L.-B. Hsin, C. R. C. Wang, S. Mann, *Chem. Commun.* **2001**, 1264.
[9] F. Kim, S. Kwan, J. Akana, P. D. Yang, *J. Am. Chem. Soc.* **2001**, *123*, 4360.
[10] Q. Lu, F. Gao, D. Zhao, *Angew. Chem. Int. Ed.* **2002**, *41*, 1932.
[11] a) J. Y. Lao, J. G. Wen, Z. F. Ren, *Nano Lett.* **2002**, *2*, 1287. b) J. Y. Lao, J. Y. Huang, D. Z. Wang, Z. F. Ren, *Nano Lett.* **2003**, *3*, 235. c) H. Q. Yan, R. R. He, J. Johnson, M. Law, R. J. Saykally, P. D. Yang, *J. Am. Chem. Soc.* **2003**, *125*, 4728.
[12] H. Shi, L. Qi, J. Ma, H. Cheng, *J. Am. Chem. Soc.* **2003**, *125*, 3450.
[13] Z. W. Pan, Z. R. Dai, Z. L. Wang, *Science* **2001**, *291*, 1947.
[14] S.-H. Yu, M. Antonietti, H. Cölfen, M. Giersig, *Angew. Chem. Int. Ed.* **2002**, *114*, 2462.
[15] P. Gao, Z. L. Wang, *J. Phys. Chem. B* **2002**, *106*, 12653.
[16] M.-P. Pileni, *Nat. Mater.* **2003**, *2*, 145.
[17] B. A. Simmons, S. Li, V. T. John, G. L. McPherson, A. Bose, W. Zhou, J. He, *Nano Lett.* **2002**, *2*, 263.
[18] H. Shi, L. Qi, J. Ma, H. Cheng, *Chem. Commun.* **2002**, 1704.
[19] a) S.-H. Yu, H. Cölfen, M. Antonietti, *Chem. Eur. J.* **2002**, *8*, 2937. b) S.-H. Yu, H. Cölfen, M. Antonietti, *Adv. Mater.* **2003**, *15*, 133. c) S.-H. Yu, M. Antonietti, H. Cölfen, J. Hartmann, *Nano Lett.* **2003**, *3*, 379.
[20] H. Cölfen, S. Mann, *Angew. Chem. Int. Ed.* **2003**, *42*, 2350.

Ultralong, Well-Aligned Single-Walled Carbon Nanotube Architectures on Surfaces**

By *Shaoming Huang*, *Benjamin Maynor*, *Xinyu Cai*, and *Jie Liu**

Single-walled carbon nanotubes (SWNTs) are ideal systems for investigating fundamental electronic properties and they are promising building blocks for molecular electronics because of their small size, unique low-dimensional structure, and electronic properties.[1,2] Although a few nanoelectronic devices based on individual SWNTs, such as quantum wires,[3] logic gates,[4] field emitters,[5] field-effect transistors,[6–8] diodes,[9] and inverters[10] have been demonstrated, there still exist two major challenges for large-scale integration of nanotube-based technology into functional electronic devices. Firstly, individual SWNTs need to be organized into rational architectures on surfaces with large-scale control of location and orientation. Additionally, because nanotubes can be semiconducting or metallic depending on their helicity and diameter, size- and structure-specific fabrication methods must be developed. While little progress has been made toward selective synthesis of metallic and semiconducting nanotubes, some progress has recently been made toward diameter control of individual SWNTs with monodisperse nanoparticles[11,12] and toward oriented growth of nanotubes directly on Si wafers by means of electric fields.[13–15]

Compared with other growth methods for SWNTs, direct chemical vapor deposition (CVD) surface growth is an inexpensive method to create isolated SWNTs with a low defect density on surfaces. Nanotubes fabricated by laser ablation and arc discharge are initially synthesized as bundles and have to be purified and suspended in solution before deposition onto a surface for device fabrication. These post-synthetic treatments may introduce defects and alter the electrical properties of SWNTs, because highly oxidative chemicals and ultrasonication processes are required for purification, suspension, and deposition. In situ CVD growth of SWNTs on surfaces either by dispersed or patterned catalysts without the aid of external forces, such as electric fields, normally yields short and randomly oriented nanotubes.[16–19] Recently, we have developed a novel CVD method to grow ultralong, well-aligned SWNTs on surfaces by rapidly heating Fe/Mo catalyst nanoparticles in the presence of a CO/H_2 feeding gas.[20] The growth direction of these nanotubes was found to be parallel to the flow direction of the feeding gas. Simply by orienting

[*] Prof. J. Liu, Dr. S. Huang, B. Maynor, X. Cai
Chemistry Department, Duke University
Durham, NC 27708 (USA)
E-mail: j.liu@duke.edu

[**] The authors would like to thank Prof. Younan Xia for the PDMS stamps used for microcontact printing. BWM acknowledges the Bill and Melinda Gates Foundation for a Gates Millenium Scholarship. This project is partially supported by a grant from NASA(NAG-1-01061), ARO(DAAD19-00-1-0548) and the 2002 Young Professor Award from DuPont.

 DOI: 10.1002/adma.200305203